Journal of Materials Chemistry B

PAPER

Pristine carbon nanotube scaffolds for the growth of chondrocytes

Cite this: DOI: 10.1039/c7tb02065a

Alice A. K. King,* [a] Brigitta Matta-Domjan, [bc] Matthew J. Large, [a] Csaba Matta, [bd] Sean P. Ogilvie, [a] Niki Bardi, [e] Hugh j. Byrne, [f] Anvar Zakhidov, [g] Izabela Jurewicz, [e] Eirini Velliou, [c] Rebecca Lewis, [b] Roberto La Ragione [b] and Alan B. Dalton [a]

Received 1st August 2017,
Accepted 5th October 2017

DOI: 10.1039/c7tb02065a

rsc.li/materials-b

The effective growth of chondrocytes and the formation of cartilage is demonstrated on scaffolds of aligned carbon nanotubes; as two dimensional sheets and on three dimensional textiles. Raman spectroscopy is used to confirm the presence of chondroitin sulfate, which is critical in light of the unreliability of traditional dye based assays for carbon nanomaterial substrates. The textile exhibits a very high affinity for chondrocyte growth and could present a route to implantable, flexible cartilage scaffolds with tuneable mechanical properties.

Introduction

Due to its lack of vascularization, cartilage is inherently limited in its ability to repair itself.[1,2] The need for synthetic materials that can be used either *in vivo* or *in vitro* to enhance or synthetically grow cartilage are therefore in high demand.[3] Nanoscale morphology has been identified as a key parameter in the development of scaffolds for tissue engineering.[4] The complex structure of cartilage has been difficult for tissue engineers to replicate and to date there are only a few examples of synthetic scaffolds that have been able to adequately encourage chondrocyte growth.[5,6] The most effective scaffolds have been derived from native cartilage, or polymer structures coated with natural proteins and polysaccharides such as collagen or chitosan.[7,8] These scaffolds are inevitably hindered by inclusion of natural materials, which vary by batch, and require extraction from animal models and post processing to produce sterile structures for culturing or implantation. Carbon nanotubes (CNTs) and their assemblies have been identified as potentially biocompatible substrates due to their morphology on the scale of cell adhesion sites.[9,10] Studies have shown that they can encourage the growth of chondrocytes, particularly under electrical stimulation.[11] Previous CNT structures have made use of CNT alignment,[12] although these CNTs have often to be pretreated to add functionalization for cell growth[13–16] or used in composites.[17–20] There has been little investigation of the interaction of pristine CNT structures with chondrocytes, mostly due to the difficulties associated with processing CNTs into 3 dimensional scaffolds without chemical treatment or hybridisation. In this study, a completely synthetic scaffold is produced from pristine CNTs eliminating the need for chemical processing, which is intrinsically *ad hoc*. The use of vibrational spectroscopy is also developed for more accurate material characterization on nanostructured substrates.

Results and discussion

The CNTs are grown as an aligned forest using the chemical vapour deposition (CVD) method and then drawn to produce an aligned sheet of CNTs. The sheet can be used as a two-dimensional cell culture substrate or twisted into fibres that can be woven into hierarchical 3-dimensional scaffolds (Fig. 1). A single forest can produce several hundred metres of sheet or fibre and so provides a simple and efficient production method. Most importantly, no chemical treatments are required. The spinning and weaving process, although completed by hand for this study, is an easily scalable process.

The chondrocytes grow and proliferate on the CNT scaffolds as shown in Fig. 2. The primary constituent of cartilage is collagen type II, and as can be seen from immunocytochemical staining (Fig. 2) production is similar for samples with the CNT substrate as for the control groups. There appears to be lower

[a] Materials Physics, University of Sussex, Brighton, UK. E-mail: alice.king@sussex.ac.uk
[b] School of Veterinary Medicine, University of Surrey, Guildford, UK
[c] Department of Chemical and Process Engineering, University of Surrey, Guildford, UK
[d] Department of Anatomy, Histology and Embryology, Faculty of Medicine, University of Debrecen, Debrecen, Hungary
[e] Department of Physics, University of Surrey, Guildford, UK
[f] Focas Research Institute, Dublin Institute of Technology, Dublin, Republic of Ireland
[g] Nanotech Institute, University of Texas at Dallas, USA

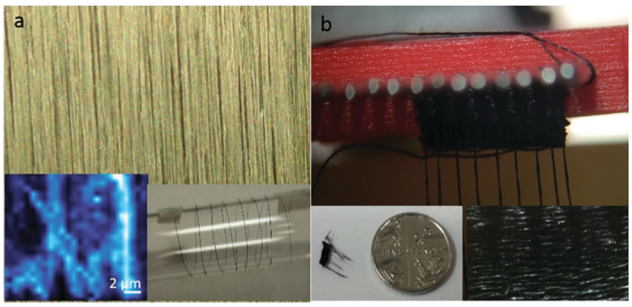

Fig. 1 Aligned CNT substrates (a) aligned aerogel sheet with inset to show the Raman map of the G peak (characteristic CNT peak at ≈ 1585 cm^{-1}) intensity of the CNTs and a twisted fibre after spinning, (b) plain weave textiles, inset to show close up and with a five pence piece for scale.

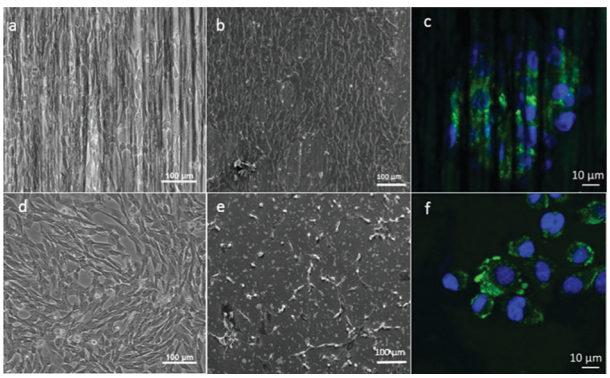

Fig. 2 Chondrocyte growth on flat, aligned CNT arrays (a–c) and controls (d–f). (a and d) Optical micrographs on day 4 (b and e) SEM images of growth after 6 days, (c and f) confocal fluorescence images, primary anti-collagen type II antibodies were visualised using Alexa488-conjugated anti-rabbit secondary antibodies (green). Nuclear DNA was stained with DAPI (blue).

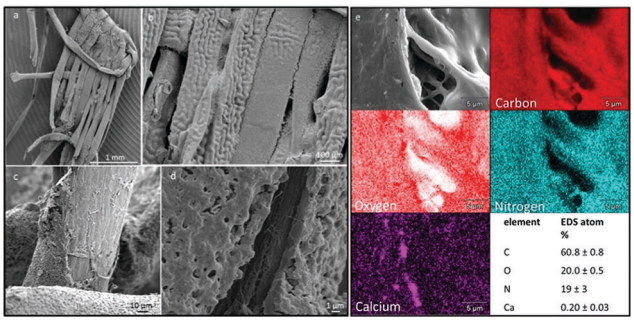

Fig. 3 SEM images of woven CNT textile, 6 days after seeding with chondrocytes (a) overview of a piece of the textile covered with cartilage, (b) the cartilage can be seen to coat the individual fibres within the textile before expanding across to form a continuous layer (c) CNT fibre exposed at the edge of the textile, (d) a crack in the cartilage reveals the CNT fibre within, (e) SEM image with EDS elemental map overlays and composition.

cell proliferation for the substrates initially which is to be expected, as cells that are functioning as chondrocytes, producing extracellular matrix (ECM), are likely to proliferate more slowly than cells cultured on standard 2D culture scaffolds. Traditional proliferation tests, such as MTT, have proven to be unreliable, as the carbon nanotubes interact strongly with the dye and modify the fluorescence.[21–24] The cell growth is often observed to be aligned with the axial direction of the CNTs; this indicates that the cytoskeleton is interacting directly with the CNT substrate. Alignment may provide some insight into the production of collagen and other ECM macromolecules in these systems, as the scale of the CNT bundles is similar to that of the collagen fibres within a cartilage tissue. A single collagen fibril is 1.5 nm in diameter and 300 nm long, with the units in a fibre staggered by 67 nm.[25] The scales of the collagen fibrils and fibres are therefore within the same regime as the individual CNTs and bundles and so chondrocytes in contact with the aligned CNT bundles mimic the native ECM around themselves. This mimicry leads to the maintenance of the chondrocyte phenotype and expression of cartilage-specific ECM components on these scaffolds.

Woven fibre textiles have been demonstrated in the literature to present a good mechanical substructure for chondrocyte growth, providing a scaffold with similar mechanical response to that of natural cartilage.[26–28] These scaffold structures have proven to be some of the most effective. The fabrication of a woven, pristine CNT textile provides some insight into the morphological response of the chondrocytes to the scaffold structure. The textiles fabricated in this work from CNT fibres showed a particularly strong affinity for the growth of chondrocytes. After only 6 days in culture the textiles were coated in cartilage-like, ECM material. The coating was across almost the entire textile and was several microns thick. The structure under SEM is highly similar to that of natural cartilage derived from animal models[29] (Fig. 3).

Raman spectroscopy has long been the standard tool for the characterisation of carbon nanomaterials, and it has been proven to be an increasingly powerful tool for the understanding of tissue culture.[30] It is particularly sensitive to variation in the ECM structure, including changes due to substrate interactions and even cancerous phenotype.[31–33] This type of structural identification is particularly important for the cartilage and bone, which are defined by the specific ECM.[34–39] The Raman spectra from three regions of the post-growth textile are presented in Fig. 4. The characteristic D, G and 2D peaks of the carbon nanotubes can be seen, unfortunately, due to the nature of the carbon bonds, the CNT peaks overlap with the amide bands in both the FTIR and Raman spectroscopy, however the peaks at lower wavenumbers are clearly distinguishable. The energy dispersive spectroscopy (EDS) (Fig. 3) shows the deposited material is composed of carbon, nitrogen and oxygen, in roughly the ratios that are found in collagen.[25] The Raman and IR spectra indicates the presence of collagen and more importantly chondroitin sulfate (CS), the primary glycosaminoglycan found in cartilage (the peak assignments are listed in Table 1).[35,39,40] It can be seen that in some regions there appears to be calcification, although EDS indicates that these are most likely deposits rather than crystallites within the structure, and the intensity is significantly lower than the CS signal. Importantly, there are two Raman peaks that are unique to healthy cartilage, the CS peaks at 937 cm^{-1} and at ≈1060 cm^{-1} respectively. These peaks are present in all the spectra

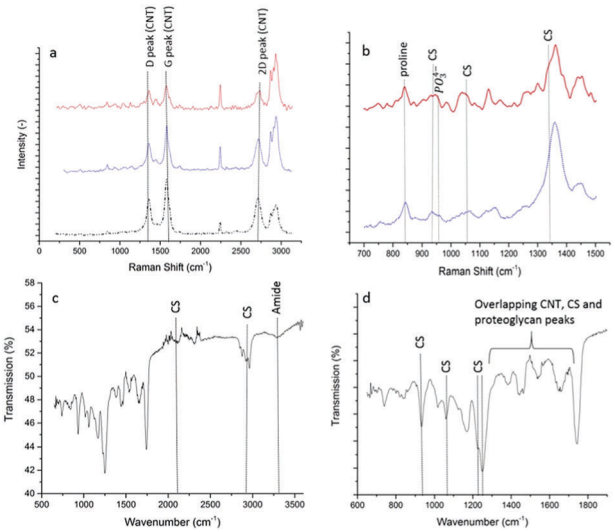

Fig. 4 Vibrational spectroscopy of ECM material (a) Raman spectra from three different regions with characteristic CNT peaks identified, (b) close up of region of interest from two regions with prescient peaks labelled, (c and d) FT IR spectroscopy with a close up of the region of interest.

taken across the textile. There are also two peaks that are indicative of calcification, at 958 cm^{-1} and 1070 cm^{-1} respectively, although these peaks are present in some spectra, these peaks are not consistently present in all areas. Therefore it seems highly likely that this deposition is cartilage grown *in vitro*. The use of Raman and FTIR to identify the cellular deposits is critical, as many traditional fluorescence based techniques are not reliable for nanomaterial substrates, especially carbon nanotubes.[21–24] The fabric-like nature of these substrates would make them ideal candidates for implants, especially across defects as they can be designed to fit in a specified region and they should be robust enough to be manipulated and to withstand the *in vivo* environment.

Experimental

Substrate preparation

The CVD forests are provided by University of Texas at Dallas. They are multiwalled forests grown *via* CVD as described in ref. 41–43. The forests are used as received and are either drawn as a single aligned sheet for the 2D substrates, or attached to a rotating motor which is drawn and twisted to create fibres. The fibres are used as is, or woven into a textile. The aligned sheet is attached to the glass substrate using a polydimethylsiloxane (PDMS) layer.

Cell culture

Cartilage was removed from the stifle and elbow condyles of skeletally mature Staffordshire bull terrier types, euthanised for unrelated veterinary reasons. Chondrocytes were isolated as described previously with type II collagenase.[44] Primary canine chondrocytes (PCCs) were cultured in low-glucose Dulbeccos Modified Eagle Medium (DMEM) containing GlutaMAX I and sodium pyruvate (Thermo Fisher Scientific, Waltham, MA USA) supplemented with 11.3 mg mL^{-1} sucrose (Sigma-Aldrich Ltd Dorset, England) in a humidified incubator at standard culture conditions (37 C, 5% CO_2) for a maximum passage number of four. Osmolality of medium was 380 mOsm. Cells were subcultured every 3 or 4 days by rinsing the monolayer cultures in sterile phosphate buffer saline (PBS; Oxoid, Basingstoke, UK), then dissociated using sterile trypsin- EDTA (Sigma-Aldrich). For microscopy and immunocytochemistry, PCCs in low passage number (P:1–P:4) were seeded onto either CNT-coated and uncoated (control) glass coverslips (borosilicate, 18 × 18 mm, 0.13–0.17 mm thick; Thermo Scientific) or onto woven CNT textiles at an initial density of 20 000 cells per well in 6-well culture plates (NUNC, Thermo Fisher Scientific) containing 3 mL of culture medium. Cell cultures were maintained on 2D CNT scaffolds and uncoated control glass coverslips for 4 days; for scanning electron microscopy 6 day-old cultures were used. After four or six days of culture cells were rinsed in PBS and fixed in 4% formaldehyde (Thermo Fisher) dissolved in PBS.

Characterisation

Immunocytochemistry was performed to visualise the production of collagen type II in 4-day old cultures of PCCs seeded onto glass coverslips coated with aligned CNT. PCCs cultured on uncoated glass coverslips were used as control. Cultures were fixed in 4% formaldehyde dissolved in PBS. After rinsing in PBS, cellular membrane was permeabilised in PBS supplemented with 2.5% bovine serum albumin (Sigma-Aldrich) and 0.75% Triton X-100 (Sigma-Aldrich), nonspecific binding sites were blocked with PBS supplemented with 5% bovine serum albumin, then cultures were incubated with rabbit polyclonal anti-collagen II primary antibody (Abcam, Cambridge, UK), at a dilution of 1 : 250 at 4 °C overnight. For visualisation of the primary antibody, anti-rabbit Alexa Fluor 488 conjugate secondary antibody (Thermo Fisher Scientific) was used at a dilution of 1 : 1000. Specificity

Table 1 Raman features of chondrocyte seeded textile after 6 days growth

Assignment	Reference values[35,39]	Area 1 (cm^{-1})	Area 2 (cm^{-1})	Area 3 (cm^{-1})
Collagen, non-cartilagenous proteins	816	817	814	—
Collagen, proline	850	841	845	845
Chondroitin sulfate C–O–C	937	938	932	938
OSO_3^-	1058–1064	1054	1054–1064	1057
	1275	1260 (shoulder)	—	1270
	1380	1385	Overlap D peak	Overlap D peak
Calcified cartilage (PO_4^{3-})	959	—	958	—
(CO_3^{2-})	1070	1080	—	—
Amide I	1660–1670	Overlap G peak	Overlap G peak	Overlap G peak
Amide II	1554	Overlap G peak	Overlap G peak	Overlap G peak
Amide III	1245–1270	1250	1255	—

of secondary antibody was confirmed by staining cells cultured on the same CNT scaffold; in these experiments, no a-specific signals were detected (data not shown). Cultures were mounted in Vectashield mounting medium (Vector Laboratories, Peterborough, England) containing 1.5 g mL^{-1} DAPI for nuclear counterstaining. Immunofluorescence confocal imaging was performed using a Nikon A1M Confocal Microscope (Nikon Corporation, Tokyo, Japan). Images were acquired using NIS Elements acquisition soft- ware. 405 and 488 nm lasers were used to excite DAPI (nuclei in blue) and Alexa488 conjugated secondary antibody detecting anti-collagen type II (green), respectively, in both treated and control samples. Emission signals were detected through 450/50 and 525/50 filters for blue and green channels, respectively. Images were captured using a planapochromat 40 × air or 60 × oil objectives. All images were processed by using the NIS Elements package (Nikon) and Photoshop software. Pinhole size was 39.6 μm. All confocal data sets were of scan zoom of 1, and line averaged eight times.

Phase contrast microscopy was performed by a Nikon DS Vi1-U2 camera on a Nikon TS100 inverted microscope (Nikon Corporation, Tokyo, Japan) with four-day old culture of PCC cells. All images were captured at a 1600 × 1200 resolution using a 10/0.25 NA air objective. Exposure time was 100 ms. For image acquisition and processing, NIS Elements F 3.0 software package (Nikon, Tokyo, Japan) was used.

Raman spectroscopy was carried out on an NT-MDT spectroscope, using 473 nm laser excitation and a ×20 objective for all flat samples. Textile was analysed using the same laser but a ×100 objective. 40 s exposures were used for all polarisation spectra and 20 s exposure for the textiles averaged over 10 spots. SEM was carried out with a Jeoul SEM with 10 kV accelerating voltage, EDS was collected over 6 min cycles using NSS spectral scanning software. Samples were gold coated. FTIR microscopy was performed using a Perkin Elmer Spotlight 400n FTIR microscope. The sample was mapped over different regions, with spectra accumulated 10 times at each point.

Conclusions

Primary chondrocytes are seen to grow and align on pristine CNT arrays in two-dimensions and to express high levels of ECM materials when cultured on 3D textiles composed of aligned CNT fibres. The ECM material is identified from Raman spectra as cartilage from the presence of chondroitin sulfate and collagen peaks. The scaffolds are entirely synthetic and un-functionalised, dictating that the growth is due to a suitable morphological structure from the CNTs, rather than a chemically mediated response.

Conflicts of interest

Q4

Acknowledgements

This work was supported by the Surrey Impact Acceleration Awards (IAA) grant no. 2015/KN9149C and grant no. 2015/K031562/1 + G060878. I. Jurewicz is supported by EPSRC grant no: EP/K031562.

References

1 E. Hunziker, *Adv. Mater.*, 2009, **21**, 3419–3424.
2 C. Sharma, S. Gautam, A. Dinda and N. Mishra, *Adv. Mater. Lett.*, 2011, **2**, 90–99.
3 D. Hutmacher, *Biomaterials*, 2000, **21**, 2529–2543.
4 B. Boyan, T. Hummert, D. Dean and Z. Schwartz, *Biomaterials*, 1996, **17**, 137–146.
5 E. Place, N. Evans and M. Stevens, *Nat. Mater.*, 2009, **8**, 457–470.
6 E. Kon, G. Filardo, A. Roffi, L. Andriolo and M. Marcacci, *Curr. Rev. in Musculoskelet. Med.*, 2012, **5**(3), 236–243.
7 J.-K. Francis Suh and H. Matthew, *Biomaterials*, 2000, **21**(24), 2589–2598.
8 W.-B. Tsai, W.-T. Chen, H.-W. Chien, W.-H. Kuo and M.-J. Wang, *Acta Biomater.*, 2011, **7**(12), 4187–4194.
9 E. Heister, E. Brunner, G. Dieckmann, I. Jurewicz and A. Dalton, *ACS Appl. Mater. Interfaces*, 2013, **5**(6), 1870–1891.
10 T. Trzeciak, J. D. Rybka, E. M. Akinoglu, M. Richter, J. Kaczmarczyk and M. Giersig, *J. Nanosci. Nanotechnol.*, 2016, **9**(16), 9022–9025.
11 D. Khang, G. Park and T. Webster, *J. Biomed. Mater. Res., Part A*, 2008, **86**(1), 253–260.
12 C. Che Abdullah, C. Lewis Azad, R. Ovalle-Robles, S. Fang, M. Lima, X. Lepr, S. Collins, R. Baughman, A. Dalton, N. Plant and R. Sear, *ACS Appl. Mater. Interfaces*, 2014, **6**(13), 10373–10380.
13 E. Anatonioli, A. O. Lobo, M. Ferretti, M. Cohen, F. R. Marciano, E. J. Corat and V. J. Trava-Airoldi, *Mater. Sci. Eng., C*, 2013, **33**, 641–647.
14 M. Machado, A. Lobo, F. Marciano, E. Corat and M. Corat, *Mater. Sci. Eng., C*, 2015, **48**, 365–371.
15 N. Chahine, N. Collette, C. Thomas, D. Genetos and G. Loots, *Tissue Eng., Part A*, 2014, **20**(17–18), 2305–2315.
16 C. Sacchetti, R. Liu-Bryan, A. Magrini, N. Rosato, N. Bottini and M. Bottini, *ACS Nano*, 2014, **8**(12), 12280–12291.
17 E. Hirata, M. Uo, Y. Nodasaka, H. Takita, N. Ushijima, T. Akasaka, F. Watari and A. Yokoyama, *J. Biomed. Mater. Res., Part B*, 2010, **93**(2), 544–550.
18 A. Doulabi, K. Mequanint and H. Mohammadi, *Materials*, 2014, **7**(7), 5327–5355.
19 S. Ilbasmis-Tamer, H. Ciftci, M. Turk, T. Degim and U. Tamer, *Curr. Pharm. Biotechnol.*, 2017, **4**(18), 327–335.
20 Y. Chen, B. Bilgen, R. A. Pareta, A. J. Myles, H. Fenniri, D. M. Ciombor, R. K. Aaron and T. J. Webster, *Tissue Eng., Part C*, 2010, **16**, 1233–1243.
21 A. Casey, E. Herzog, M. Davoren, F. M. Lyng, H. J. Byrne and G. Chambers, *Carbon*, 2007, **45**, 1425–1432.
22 N. A. Monteiro-Riviere, A. O. Inman and L. W. Zhang, *Toxicol. Appl. Pharmacol.*, 2009, **234**, 222–235.
23 J. Worle-Knirsch, K. Pulskap and H. Krug, *Nano Lett.*, 2006, **6**(6), 1261–1268.

24 S. H. Doak, S. M. Griffiths, B. Manshian, N. Singh, P. M. Williams, A. P. Brown and G. J. S. Jenkins, *Mutagenesis*, 2009, **24**(4), 285–293.

25 *Collagen: Structure and Mechanics*, ed. P. Fratzl, Springer, 2008.

26 F. Moutos, L. Freed and F. Guilak, *Nat. Mater.*, 2007, **6**(2), 162–167.

27 I.-C. Liao, F. Moutos, B. Estes, X. Zhao and F. Guilak, *Adv. Funct. Mater.*, 2013, **23**(47), 5833–5839.

28 S. McCullen, C. Haslauer and E. Loboa, *J. Mater. Chem.*, 2010, **20**(40), 8776–8788.

29 H. Stein and D. Levanon, *J. Anat.*, 1998, **192**(3), 343–349.

30 M. s. Dresselhaus, G. Dresselhaus, R. Saito and A. Jorio, *Phys. Rep.*, 2005, **409**(2), 47–99.

31 A. Kunstar, A. Leferink, P. Okagbare, M. Morris, B. Roessler, C. Otto, M. Karperien, C. Van Blitterswijk, L. Moroni and A. Van Apeldoorn, *J. R. Soc., Interface*, 2013, **10**(86.

32 A. Daniel, A. Prakasarao, K. Dornadula and S. Ganesan, *Spectrochim. Acta, Part A*, 2015, **152**, 58–63.

33 K. Klein, A. Gigler, T. Aschenbrenner, R. Monetti, W. Bunk, F. Jamitzky, G. Morfill, R. Stark and J. Schlegel, *Biophys. J.*, 2012, **102**(2), 360–368.

34 M. Pudlas, E. Brauchle, T. Klein, D. Hutmacher and K. Schenke-Layland, *J. Biophotonics*, 2013, **6**(2), 205–211.

35 J. Mansfield, J. Moger, E. Green, C. Moger and C. Winlove, *J. Biophotonics*, 2013, **6**(10), 803–814.

36 S. Gamsjaeger, K. Klaushofer and E. Paschalis, *J. Raman Spectrosc.*, 2014.

37 N. Lim, Z. Hamed, C. Yeow, C. Chan and Z. Huang, *J. Biomed. Opt.*, 2011, **16**(1).

38 G. Falgayrac, S. Facq, G. Leroy, B. Cortet and G. Penel, *Appl. Spectrosc.*, 2010, **64**(7), 775–780.

39 A. Bonifacio, C. Beleites, F. Vittur, E. Marsich, S. Semeraro, S. Paoletti and V. Sergo, *Analyst*, 2010, **135**, 3193–3204.

40 N. P. Camacho, P. West, P. A. Torzilli and R. Mendelsohn, *Biopolymers*, 2001, **62**, 1–8.

41 S. Fang, M. Zhang, A. Zakhidov and R. Baughman, *J. Phys.: Condens. Matter*, 2010, **22**, 33.

42 M. Zhang, S. Fang, A. A. Zakhidov, S. B. Lee, A. E. Aliev, C. D. Williams, K. R. Atkinson and R. H. Baughman, *Science*, 2005, **5738**(309), 1215–1219.

43 M. Zhang, K. R. Atkinson and R. H. Baughman, *Science*, 2004, **5700**(306), 1358–1361.

44 R. Lewis, K. Asplin, G. Bruce, C. Dart, A. Mobasheri and R. Barrett-Jolley, *J. Cell. Physiol.*, 2011, **226**(11), 2979–2986.